Pharmaceutical Sciences Asia

Pharm Sci Asia 2025; 52(4), 506-517

DOI:10.29090/psa.2025.04.25.4591

Research Article

Formulation optimization and *in vitro* and *ex vivo* evaluation of *Boesenbergia rotunda* extract-loaded microemulsion using experimental design model

Panatda Wittayanukullack[1,2], Praneet Opanasopit[1], Phuvamin Suriyaaumporn[1], Worranan Rangsimawong[2,*]

[1]Department of Industrial Pharmacy, Faculty of Pharmacy, Silpakorn University, Nakhon Pathom 73000, Thailand
[2]Division of Pharmaceutical Chemistry and Technology, Faculty of Pharmaceutical Sciences, Ubon Ratchathani University, Ubon Ratchathani, Thailand, 34190.

ABSTRACT

Boesenbergia rotunda (L.) extract is characterized by the presence of pinostrobin (PNS) as its major active component. PNS expresses several pharmacological activities such as antioxidant, anti-inflammatory, antiviral, anticancer, and anti-aromatase activities. Similar to other flavonoids, PNS has poor water solubility, resulting in low bioavailability and limiting its clinical application. These physicochemical constraints pose significant challenges for effective transdermal delivery, particularly in achieving sufficient drug penetration across the stratum corneum. To address these limitations, the development of an effective drug delivery system that can improve both the solubility and transdermal permeation of PNS is warranted. This study aimed to develop an optimized microemulsion (ME) formulation for the transdermal delivery of *B. rotunda* extract, focusing on PNS. Various oils, surfactants, and co-surfactants were screened, and different surfactant to co-surfactant ratios were evaluated through pseudo-ternary phase diagrams and optimized using Design Expert software. The developed ME was characterized for physical appearance, droplet size, polydispersity index (PDI), zeta potential, pH, entrapment efficiency, *in vitro* release and *ex vivo* skin permeation. For the result, the optimized formulation was with a fixed surfactant to co-surfactant ratio of 3:1. The optimized ME consisted of 63.34% Labrasol® and Transcutol®, 18.33% limonene, and 18.33% water, which the mean droplet size, PDI, zeta potential and entrapment efficiency were discovered as 156.0±0.80 nm, 0.21±0.02, 0.05±0.03 mV, and 99.79%, respectively. *In vitro* drug release studies demonstrated that the ME exhibited a higher release rate than the oil solution but a lower release rate than the extract in ethanol solution over a 24-hour period. *Ex vivo* skin permeation studies revealed that the optimized ME demonstrated significantly higher skin permeation than the control formulations. In conclusion, these findings suggest that the developed ME is a promising carrier system for enhancing the transdermal delivery of PNS.

Keywords:
Boesenbergia rotunda extract; Pinostrobin; Microemulsion; Design expert

1. INTRODUCTION

Boesenbergia rotunda (L.) Mansf. (*B. rotunda*), a member of the Zingiberaceae family and commonly referred to as fingerroot or “krachai” in Thai, is a well-known medicinal and culinary herb predominantly found in tropical regions of China, South Asia, and Southeast Asia [1]. The rhizome of *B. rotunda* is used as a food ingredient in Thai cuisine and many countries. It has been utilized as a traditional medicine to treat various diseases, including gastrointestinal disorders, peptic ulcers, flatulence, dyspepsia, rheumatism, muscle pain, and fever reduction [2]. *B. rotunda* extract is rich in several bioactive compounds such as flavonoids, esters, terpenes,

***Corresponding author:**
* Worranan Rangsimawong Email: worranan.r@ubu.ac.th

Pharmaceutical Sciences Asia © 2024 by
Faculty of Pharmacy, Mahidol University, Thailand is licensed under CC BY-NC-ND 4.0. To view a copy of this license, visit https:// www.creativecommons.org/licenses/by-nc-nd/4.0/

terpenoids, and chalcone derivatives [3]. Pinostrobin (PNS) or 5-hydroxy-7-methoxyflavanone is a naturally occurring flavonoid primarily extracted from the rhizomes of *B. rotunda* [4]. PNS has gained attention due to its diverse pharmacological activities, which include antioxidant [5,6], anti-inflammation [6], anti-peptic ulcer [7], anti-cancer, anti-microbial [5], anti-viral [8,9], and anti-obesity effects [10]. Furthermore, PNS has demonstrated potential in against-osteoporosis [11], reducing estrogen-induced cell proliferation [12], neuroprotective effect [13], and anti-aromatase activities [14]. However, the feasibility of PNS in pharmacological application is limited, due to its poor water solubility and sensitivity to environmental factors, including high temperatures, light exposure, pH fluctuations, and enzymatic degradation [15]. These limitations may decrease the effectiveness and bioavailability of the bioactive compound.

Transdermal drug delivery systems (TDDS) offer an attractive alternative route for PNS administration. Compared with oral administration, TDDS can bypass gastrointestinal degradation and first-pass hepatic metabolism, thereby improving bioavailability and therapeutic effectiveness[16]. In addition, TDDS show several advantages over parenteral administration, including painless, noninvasiveness, and improve patient compliance [17]. Importantly, TDDS can provide controlled and sustained release, leading to maintain steady plasma level and potentially minimizing systemic side effects [18, 19]. Nevertheless, the stratum corneum, which constitutes the outermost layer of the skin, acts as a significant barrier that restricts the penetration of many compounds, including PNS [20]. To overcome the obstacles, the development of novel transdermal delivery strategies is being explored to enhance the solubility and skin permeation of poorly soluble bioactive, such as PNS.

In recent years, ME systems have emerged as an advanced drug delivery platform. ME are thermodynamically stable systems consisting of oil, water, surfactant, and frequently co-surfactant, which self-assemble into nano-sized droplets typically ranging from 10 to 200 nm [21]. ME have emerged as a potential approach for poorly water-soluble drugs delivery. ME significantly enhances drug solubilization by forming nano-sized droplets that provide a substantially increased surface area, thereby promoting improved absorption and bioavailability [22]. Pseudo-ternary phase diagrams are commonly employed to identify the ME region where a stable ME forms, based on the proportions of oil, surfactant and co-surfactant mixture, and water [23]. While formulations are often not specially chosen from within the region, employing experimental design models enables a systematic determination of the most optimal ME composition.

The aim of the present study was to optimize the formulation of *B. rotunda* extract-loaded ME, focusing on PNS by an experimental design model. Initially, the solubility of the extract, particularly PNS, was assessed in various oils, surfactants, and co-surfactants to determine the optimal components for ME formation. Pseudo-ternary phase diagrams were constructed to obtain the ME regions, and a simplex lattice statistical design was employed to identify the most effective formulation parameters. The optimized ME was characterized in terms of droplet size, polydispersity index (PDI), zeta potential, and entrapment efficiency. Moreover, *in vitro* release profile and *ex vivo* skin permeation properties of PNS were investigated.

2. MATERIALS AND METHODS

2.1. Materials

The ethanolic extract of *B. rotunda* (L.) Mansf. was obtained from the Faculty of Pharmaceutical Sciences, Ubon Ratchathani University, Thailand [24]. Quantitative analysis by HPLC revealed a PNS content of 452 mg/g of the crude extract. PNS standard and d-limonene were purchased from Sigma-Aldrich Co. (St. Louis, MO, USA). Caprylocaproyl Polyoxyl–8 glycerides (Labrasol®) was kindly gifted by Gattefossé Co. (Paramus, NJ, USA). Ethoxydiglycol (Transcutol® CG) was purchased from Chanjao Longevity Co., Ltd. (Bangkok, Thailand). Acetonitrile was from Fisher Scientific (Seoul, Korea). Ortho-phosphoric acid, absolute ethanol (99.9%) and methanol were acquired from Merck & Co. (Darmstadt, Germany). All other chemicals and solvents were of analytical reagent grade.

2.2. Solubility study

The solubility of PNS, derived from *B. rotunda* extract in various oils, surfactants and co-surfactants was evaluated as summarized in Table 1. An excess amount of the extract was added to 1 mL of each solvent, and the mixtures were shaken at 25 °C 150 rpm for 72 h. The saturated samples were centrifuged at 14,000 rpm for 20 min. The supernatant was collected, and the solubility of PNS was determined by high-performance liquid chromatography (HPLC). The solvents, including oil, surfactant, and co-surfactant, that provide the maximum solubility of PNS were selected for further studies.

To determine the solubility of PNS in the optimized ME, an excess amount of *B. rotunda* extract was added to the 1 mL of the optimized ME formulation. The mixture was shaken at 25 °C 150 rpm for 72 h, followed by centrifugation at 14,000 rpm for 20 min. The supernatant was then analyzed for PNS content using HPLC.

Table 1. Types of oils, surfactants, and co-surfactants used in the study

Oils	Surfactants	Co-surfactants
Oleic acid	Tween® 20	Ethanol
D-limonene	Tween® 80	PEG400
Eugenol	Brij® O10	Propylene glycol
Winter green oil	Brij® 93	Transcutol®
Peppermint oil	Labrasol®	
Rice bran oil	Labrafil® M 144 CS	
Coconut oil	Cremophor RH40	
Almond oil		
Olive oil		
Medium chain triglycerides (MCT)		
Labrafac® PG		

2.3. HPLC condition

The HPLC analytical conditions used in this study were adapted from previously published methods for the quantification of *B. rotunda* extract [24,25]. The HPLC system consisted of a pump (Thermo Scientific™ Dionex™ UltiMate 3000 System, Germering, Germany), VertiSep™ GES C18 column (4.6 × 250 mm, 5 µm; Vertical Chromatography Co., Ltd., Bangkok, Thailand) and a UV detector set at 285 nm. The mobile phase consists of a gradient system of acetonitrile and phosphoric acid (0.1% v/v), starting with 20% acetonitrile and reaching 80% in the final phase. The flow rate was maintained at 1.5 mL/min, with a total run time of 60 minutes. Under these conditions, the retention time of PNS was approximately 44 minutes.

2.4. Construction of the pseudo-ternary phase diagrams

Pseudo-ternary phase diagrams were fabricated using the aqueous titration technique to determine the ME formation region. The system consisted of three major components: oil phase, aqueous phase (distilled water), and emulsifier phase. The emulsifier phase was prepared by mixing surfactant (S) and co-surfactant (CoS) at different weight ratios (3:1, 2:1, 1:1, and 1:2). Each S/CoS mixture was combined with the oil phase at varying weight ratios (1:9, 2:8, 3:7, 4:6, 5:5, 6:4, 7:3, 8:2, and 9:1) in glass vials at room temperature.

Subsequently, distilled water was gradually added to each mixture using a burette under continuous stirring with a magnetic stirrer. The titration process was carried on until turbidity appeared, indicating phase separation. The visual appearance of each mixture was recorded throughout the titration process to determine the formation of either a transparent ME or a turbid non-ME.

The percentage of each component in the ternary phase system was calculated, and the phases were plotted to generate a ternary phase diagram distinguishing ME zones (clear) from non-ME zones (cloudy), using CHEMIX School software (version 12.2). The resulting diagram delineated the ME region from the non-ME region. The identified ME region served as a guide for selecting the appropriate component ratios for further experimental design and formulation optimization.

2.5. Experimental design and optimization of microemulsion formulations

To optimize the ME formulation, a mixture design approach was employed using Design-Expert® software version 13.0.5 (Stat-Ease Inc., Minneapolis, MN, USA). The experimental design followed a simplex lattice model, which is appropriate for formulations composed of multiple components that sum to a fixed total.

Three independent variables, representing the major components of the ME system, were selected: oil phase (X_1), emulsifier phase (X_2), and aqueous phase (X_3). The component limits were established according to the ME region determined from the pseudo-ternary phase diagrams. The defined constraints were as follows:

$$10 \leq X_1 \leq 30\% \quad (1)$$
$$60\% \leq X_2 \leq 80\% \quad (2)$$
$$10 \leq X_3 \leq 30\% \quad (3)$$
$$X_1 + X_2 + X_3 = 100\% \quad (4)$$

The simplex lattice design was generated under these constraints, yielding a total of 10 randomized experimental runs. Each formulation was prepared according to the predicted component ratios and evaluated for the following response variables: PDI (Y_1), droplet size (Y_2), and zeta potential (Y_3). These responses were selected as critical quality attributes (CQAs) for the characterization and performance assessment of the ME system.

The concentrations of the three formulation components were simultaneously varied using computer

design, while maintaining the total composition at a constant 100%. A total of 10 ME formulations were generated by Design-Expert® software (version 13.0.5) to investigate the relationship between the independent variables (input factors) and the measured responses (output factors), as summarized in Table 2.

Table 2. Experimental batches of *B. rotunda* extract-loaded MEs and output factors using D-optimal design

Run	Input Factor 1 X_1: Oil (% *w/w*)	Input Factor 2 X_2: S/CoS (% *w/w*)	Input Factor 3 X_3: Water (% *w/w*)	Output Factor 1 Y_1: PDI	Output Factor 2 Y_2: Size (nm)	Output Factor 3 $Y3$: Zeta potential (mV)
1	10.00	60.00	30.00	0.228	143.5	+0.0336
2	10.00	70.00	20.00	0.330	366.7	+0.0216
3	20.00	60.00	20.00	0.183	107.7	+0.0645
4	13.33	63.33	23.33	0.237	163.3	+0.0532
5	20.00	70.00	10.00	0.287	173.7	+0.0468
6	16.67	66.67	16.67	0.330	182.3	+0.0312
7	30.00	60.00	10.00	0.184	134.2	+0.0244
8	10.00	80.00	10.00	0.816	924.3	-0.0171
9	23.33	63.33	13.33	0.213	119.4	+0.0683
10	13.33	73.33	13.33	0.778	861.7	-0.0529

2.6. Formulation of *B. rotunda*-loaded microemulsions

A 5% w/w solution of *B. rotunda* extract dissolved in d-limonene was prepared using a vortex mixer. Based on the ratios suggested by the experimental design, predetermined amounts of the S/CoS mixture (Labrasol® and Transcutol®) and water were added to the mixture. The formulations were stirred for 10 minutes to achieve homogeneous mixing. Only clear and homogeneous formulations, without any precipitated crude extract, were collected and characterized.

2.7. Characterization of microemulsions

2.7.1- Droplet size, PDI, and zeta potential measurement

The droplet size, PDI, and zeta potential of the ME formulations were determined using photon correlation spectroscopy (PCS) with a Zetasizer Nano Series analyzer (Malvern Instruments, Malvern, UK). Measurements were carried out at 25 °C with a fixed scattering angle of 90°. All measurements were performed in triplicate.

2.7.2 pH value

The pH of each ME formulation was measured at room temperature using a digital pH meter (Mettler Toledo, SevenCompact™ S220, Switzerland). The measurements were conducted in triplicate.

2.7.3 Entrapment efficiency determination

The percent entrapment efficiency (%EE) of PNS in the ME was determined following previously reported protocols [26,27,28]. The entrapment of PNS from *B. rotunda* extract-loaded ME was diluted with a known volume of absolute ethanol. The extraction of PNS from the ME was centrifuged at 10,000 rpm at 25 °C for 10 min. The supernatant was filtered through a 0.45 µm nylon membrane filter, and the filtrate was analyzed using HPLC. The PNS concentration in the supernatant was assumed to represent the concentration of the encapsulated drug (C) [29]. The entrapment efficiency was then calculated according to the following equation:

$$\% \text{ EE} = (C/C_i) \times 100$$

Where C is the concentration of PNS in the formulation, and C_i is the initial concentration of PNS.

2.8. *In vitro* release study

The *in vitro* release profile of PNS from the ME formulation was investigated by the dialysis bag method. Two milliliters of the *B. rotunda* extract-loaded ME formulation was placed into a tightly sealed dialysis membrane (molecular weight cut-off: 6–8 kDa; Spectrum™ Spectra/Por™, Spectrum Laboratories, Inc., CA, USA). The dialysis bag was immersed in 60 mL of a release medium composed of phosphate-buffered saline (PBS, pH 7.4) with polysorbate 20 (5 g/L) and ethanol in a 1:1 (v/v) ratio with continuous stirring. At predetermined time intervals of 1, 2, 4, 6, 8, 12, and 24 h, 1.0 mL of the release medium was withdrawn and immediately replaced with an equal volume of fresh medium. The collected samples were filtered through a 0.45 µm nylon membrane filter and analyzed for PNS content using HPLC. The cumulative drug release at each time interval was calculated and plotted to construct the release profile.

2.9. *Ex vivo* skin permeation study

Abdominal porcine skin was obtained from an intrapartum stillborn piglet sourced from a local farm in Ubon Ratchathani Province, Thailand, with ethical approval for collection granted by the Investigational Review Board (27/2568/IACUC, Animal Experimentation Ethics Committee, Ubon Ratchathani University, Ubon Ratchathani, Thailand). The subcutaneous fat was carefully removed using surgical scissors, yielding skin with a thickness of approximately 600–700 µm. The skin samples were stored at −20 °C until further use.

Ex vivo skin permeation studies were conducted using vertical Franz-type diffusion cells. The receptor compartment was filled with 6 mL of PBS (pH 7.4) containing polysorbate 20 (5 g/L) and ethanol in a 1:1 ratio. The receptor medium was continuously stirred with a magnetic stirrer and maintained at 32 ± 0.5 °C. Each piece of skin was mounted between the donor and receptor compartments. Two milliliters of the test formulation were applied to the skin surface. After 24 h of the skin permeation, the receiver medium was collected for HPLC analysis. For the skin deposition study, the surface of the skin was gently rinsed, sectioned into small fragments, and subjected to extraction in ethanol using an ultrasonic bath for 30 min. The amounts of PNS that permeated through and remained deposited in the skin were quantified in triplicate using HPLC.

2.10 Statistical analysis

All data were represented as mean values ± standard deviation (S.D). Statistical analysis of differences among the tested formulations was performed using one-way ANOVA followed by Tukey's post hoc test, utilizing SPSS Statistics software version 22.0 (IBM Corp., Armonk, NY, USA). A *p*-value of less than 0.05 ($p < 0.05$) was considered statistically significant.

3. RESULTS AND DISCUSSION

3.1 Pinostrobin solubility study

The solubility of PNS was investigated in various types of oils, surfactants, and co-surfactants to identify the most appropriate components for the ME formulation. The solubility data are presented in Table 3. Among the oils, d-limonene exhibited the highest solubility of PNS at 149.99 ± 4.90 mg/mL and was selected as the oil phase. For the surfactant and co-surfactant screening, Labrasol® (138.79 ± 2.92 mg/mL) and Transcutol® (197.31 ± 2.73 mg/mL) demonstrated the highest solubility of PNS, respectively. Consequently, Labrasol® and Transcutol® were selected as the surfactant and co-surfactant, respectively, for the construction of the pseudo-ternary phase diagrams.

3.2 Pseudo-ternary phase diagrams

Pseudo-ternary phase diagrams were generated to identify the ME regions formed using d-limonene as the oil phase, Labrasol® as the surfactant, and Transcutol® as the co-surfactant at various surfactant/co-surfactant (S/CoS) weight ratios. The ratios studied included 3:1, 2:1, 1:1 and 1:2, with distilled water as the aqueous phase. The ME regions are represented in gray area in Figure 1.

The area of the ME region varied significantly depending on the S/CoS ratio. The combination of the S/CoS at a 3:1 ratio presented the largest ME region as shown in Figure 1a. At a 2:1 ratio of the S/CoS, the ME region was still considerable but smaller than the 3:1 ratio of S/CoS system. This trend continued with the 1:1 (Figure 1c) and 1:2 ratios (Figure 1d), where the ME regions became notably narrower. The presence of higher amounts of Transcutol® may increase interfacial fluidity and can disrupt the structural integrity of the interfacial film [30, 31], thereby reducing the emulsification efficiency and limiting the formation of stable MEs.

Table 3. PNS solubility in different types of oils, surfactants, and co-surfactants

Oils	Solubility (mg/mL)	Surfactants	Solubility (mg/mL)	Co-surfactants	Solubility (mg/mL)
Oleic acid	99.39 ± 1.33	Tween® 20	118.95 ± 3.72	Ethanol	122.52 ± 2.08
D-limonene	149.99 ± 4.90	Tween® 80	97.70 ± 3.50	PEG 400	99.37 ± 1.07
Eugenol	123.70 ± 2.09	Brij® O10	86.33 ± 3.66	Propylene glycol	64.18 ± 1.64
Winter green oil	90.83 ± 4 .51	Brij® 93	112.74 ± 4.33	Transcutol®	197.31 ± 2.73
Peppermint oil	126.11 ± 2.58	Labrasol®	138.79 ± 2.92		
Rice bran oil	77.10 ± 1.47	Labrafil®	106.85 ± 2.80		
Coconut oil	125.94 ± 2.90	Cremophor RH40	55.13 ± 2.70		
Almond oil	94.13 ± 4.72				
Olive oil	57.40 ± 2.76				
MCT	118.95 ± 3.72				
Labrafac®	137.45 ± 3.49				

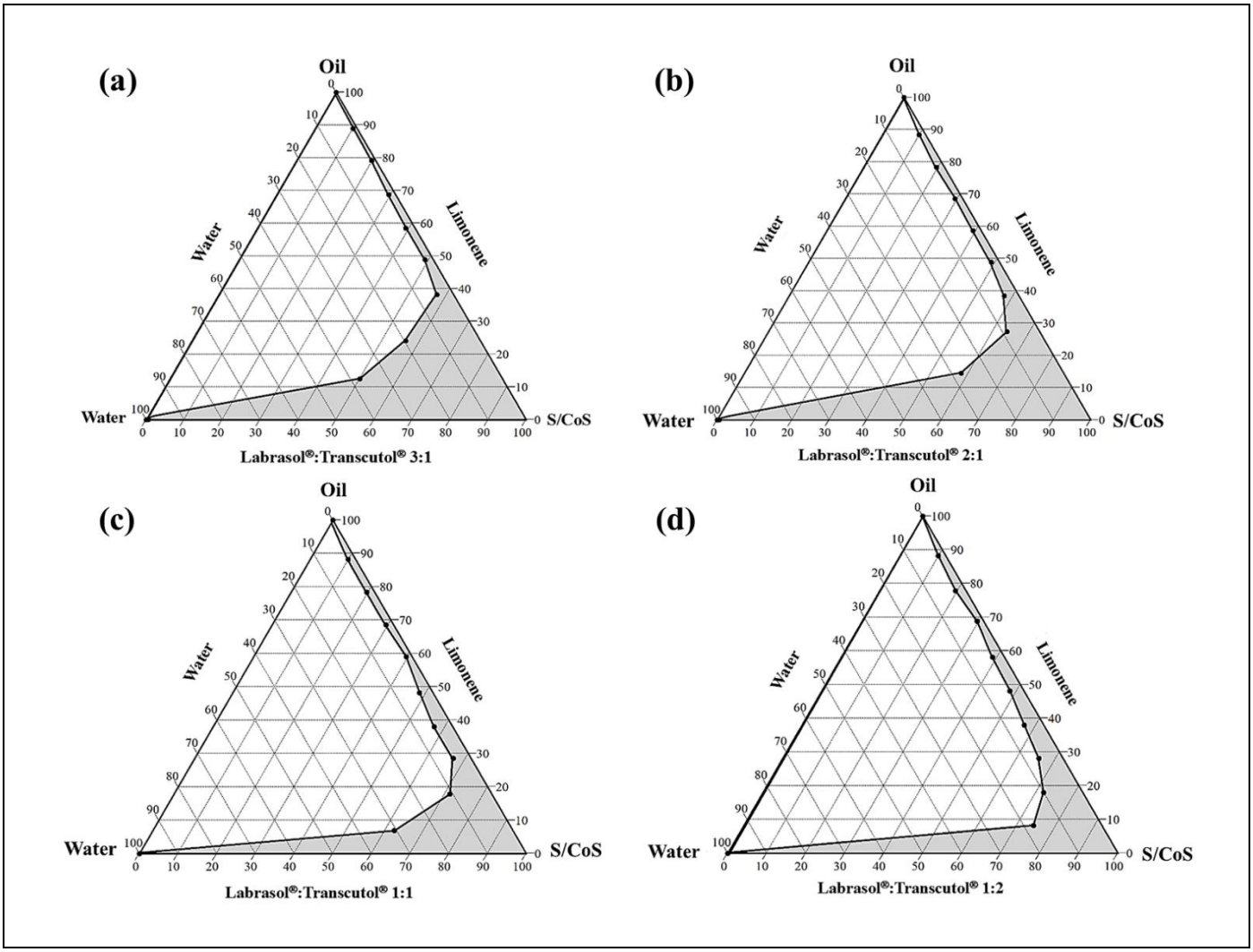

Figure 1. Pseudo-ternary phase diagrams of d-limonene, water, and various S/CoS (a) 3:1, (b) 2:1, (c) 1:1, and (d) 1:2. The ME regions are presented by the gray shaded areas.

These findings highlight the crucial role of the S/CoS balance in optimizing ME systems. While co-surfactants assist in flexibility and interface formation, a dominant surfactant ratio (3:1) appears to offer the best compromise between interfacial tension reduction and interfacial film stability. Accordingly, Labrasol® is a non-ionic surfactant which is excellent in emulsification efficiency. When used in higher proportions, it enhances the solubility of poor water-soluble compounds and produce a physically stable of ME system [32, 33]. The pseudo-ternary phase diagrams study confirmed that the system comprising d-limonene (oil), Labrasol®: Transcutol® (3:1, S/CoS), and water provided the widest ME region, suggesting the superior potential for use in the development of ME formulations. This system was selected for further formulation optimization and evaluation.

3.3 Optimization of microemulsions

The formulation components of selected MEs (with an S/CoS ratio of 3:1) were optimized using a D-optimal mixture design. The levels selected for mixture design were oil 10-30 %, S/CoS 60-80 %, and water 10-30 %, creating a total of 10 experimental runs. The results of output factors such as PDI (Y_1), droplet size (Y_2), and zeta potential (Y_3) are shown in Table 2.

In this study, the PDI of *B. rotunda* extract-loaded ME ranged from 0.183 to 0.816. The lowest PDI was observed at 20% oil, 60% S/CoS, and 20% water (Run 3), indicating a more homogenous droplet size distribution. Higher PDI values, such as in Run 10 (PDI = 0.778), were associated with increased S/CoS concentrations, possibly due to droplet coalescence or system instability as presented in the contour and 3D surface plots (Figure 2a, b). Correspondingly, droplet sizes varied from 107.7 nm to 924.3 nm. Contour and 3D plots (Figure 2c, d) revealed that higher S/CoS concentrations (X_2) tend to increase droplet size. The smallest droplet size was also shown in Run 3 (107.7 nm), indicating that balanced compositions can promote nano-scaled droplets. Larger sizes observed at higher S/CoS levels in Run 8 and 10, may be attributed to excessive surfactant concentrations, which can increase

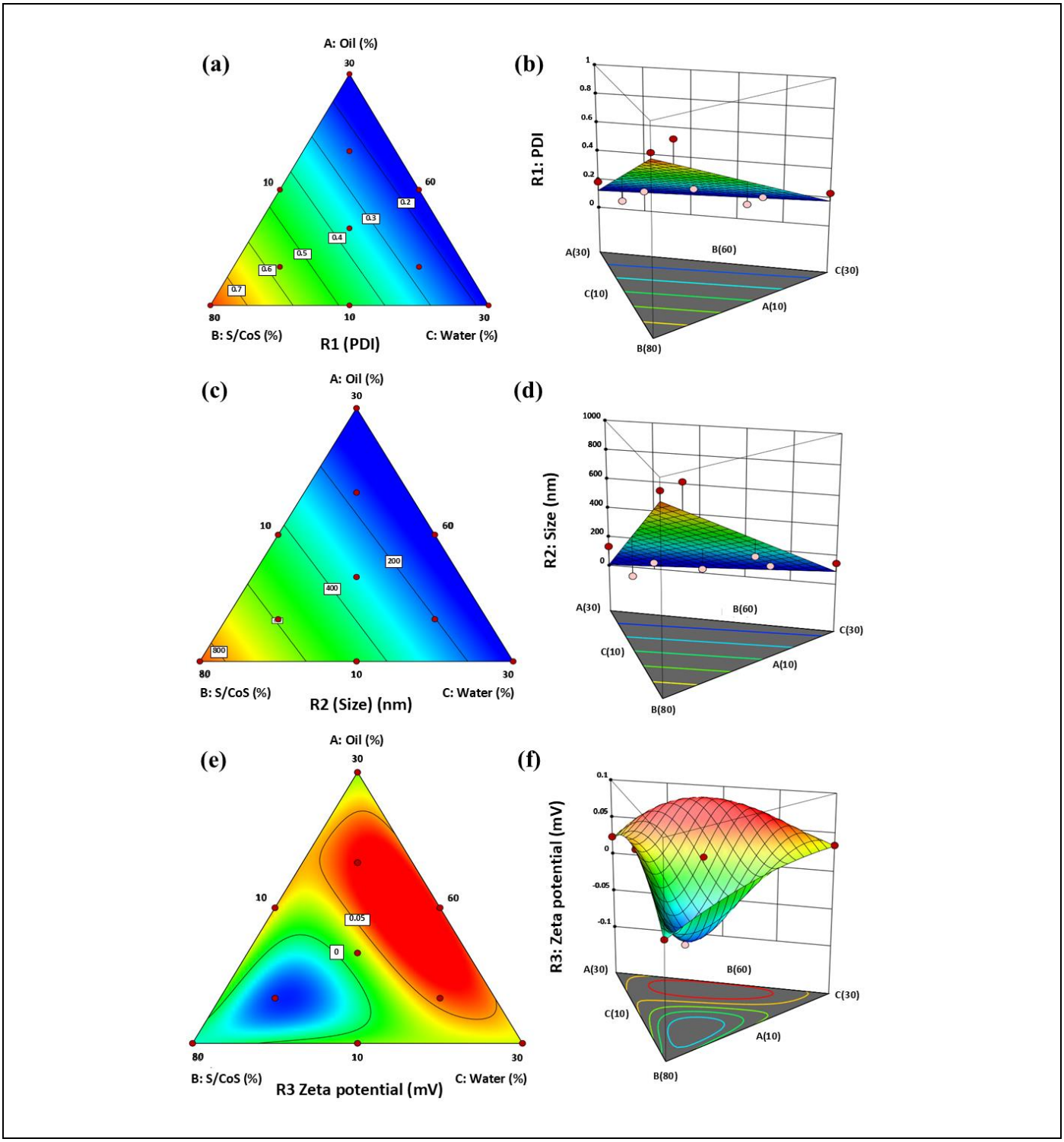

Figure 2. 2D contour plot and 3D response surface area of (a,b) PDI, (c,d) size and (e,f) zeta potential of *B. rotunda* extract-loaded ME formulations

the viscosity of the ME system and promote droplet aggregation. Moreover, zeta potential ranged from −0.0529 to +0.0683 mV, suggesting neutral surface charge behavior consistent with the use of non-ionic surfactants, Labrasol® and Transcutol®. The contour and 3D plots (Figure 2e, f) showed a tendency for higher oil and water levels to increase the zeta potential toward slightly positive values. In contrast, higher S/CoS concentration decreased the zeta potential.

To identify the optimal *B. rotunda* extract-loaded ME formulation, Design-Expert® version 13.0.5 software was employed to analyze the data using desirability-based multi-response optimization criteria, as summarized in Table 4. The optimal formulation comprised 18.33% oil (d-limonene), 63.34% S/CoS (Labrasol®: Transcutol® at 3:1), and 18.33% water, with an overall desirability score of 1.000, indicating an excellent match to the optimization goals. In general, desirability values between 0.8 and 1.0

are considered indicative of high-quality formulations, supporting the suitability of the selected composition.

To validate the optimized formulation, the predicted values were compared with the experimentally observed values, and the differences were statistically assessed using a t-test. As presented in Table 5, the experimental results showed no significant difference from the predicted values across all measured responses, confirming the reliability and accuracy of the optimization model.

Table 4. Criteria for optimized *B. rotunda* extract-loaded ME formulation

Factors	Criteria	Solutions	Desirability
X_1 Oil (%*w/w*)	is in range	18.33 %	1.000
X_2 S/CoS (%*w/w*)	is in range	63.34 %	
X_3 Water (%*w/w*)	is in range	18.33 %	
PDI	Minimize	0.2533	
Size (nm)	Minimize	181.63	
Zeta potential	None		

Table 5. Comparison between predicted and experimental values of response parameters for the optimized *B. rotunda* extract-loaded ME formulation

Results	Output Factors		
	PDI	Size (nm)	Zeta potential (mV)
Predicted value	0.391 ± 0.000	181.63 ± 0.00	+0.0828 ± 0.00
Actual value	0.219 ± 0.010	156.00 ± 0.80	+0.0312 ± 0.0186
t-test (p-value)	0.076	0.863	0.422

3.4 Characterization of microemulsions

The optimized *B. rotunda* extract-loaded ME formulation was characterized to evaluate its physicochemical properties, including droplet size, PDI, zeta potential, pH, and entrapment efficiency, as presented in Table 6.

The optimized ME formulation exhibited an average droplet size of 156.0 ± 0.80 nm, indicating nano-scaled droplet, which is favorable for transdermal delivery. The reduced droplet size enhances surface area and facilitates drug permeation across the skin barrier. The PDI was found to be 0.219 ± 0.010, reflecting a narrow and uniform droplet size distribution. This suggests good physical stability and homogeneity of formulation. Additionally, the zeta potential was +0.0312 ± 0.0186 mV, indicating a near-neutral surface charge. As expected from the use of non-ionic surfactants (Labrasol® and Transcutol®). The measured pH was 6.83 ± 0.12. Importantly, the entrapment efficiency was remarkably high at 99.79 ± 0.60%, demonstrating that this ME system is highly effective for encapsulating and retaining PNS when incorporated at 5% *B. rotunda* extract.

Table 6. Size, PDI, zeta potential, pH, and entrapment efficiency of optimized ME

Formulation	Size (nm)	PDI	Zeta potential (mV)	pH	%EE
Optimized ME	156.00 ± 0.80	0.219 ± 0.010	0.0312 ± 0.0186	6.83 ± 0.12	99.79 ± 0.60

3.5 *In vitro* drug release study

The *in vitro* drug release profile of *B. rotunda* extract-loaded ME was assessed by the dialysis bag method over 24 h. For comparison, control formulations containing the *B. rotunda* extract in ethanol and oil solutions were also examined. The cumulative drug release percentage at each time point is illustrated in Figure 3.

The *B. rotunda* extract in ethanol solution exhibited the highest cumulative drug release, reaching 14.33 ± 0.44% at 24 h. In contrast, the *B. rotunda* extract in oil solution showed minimal drug release, with only about 2.11 ± 0.38% cumulative release at 24 h. The slow-release rate from the oil phase is due to the lipophilic nature, which restricts drug diffusion across the hydrophilic dialysis membrane. The ME formulation demonstrated a moderate release profile, with cumulative drug release peaking around 8.63 ± 0.63 % at 24 h. The result demonstrated that the ME system provided a more controlled and sustained release of PNS than ethanol solution, while significantly faster release than the oil solution (p-value < 0.05). The controlled released observed from the ME formulation can be explained by

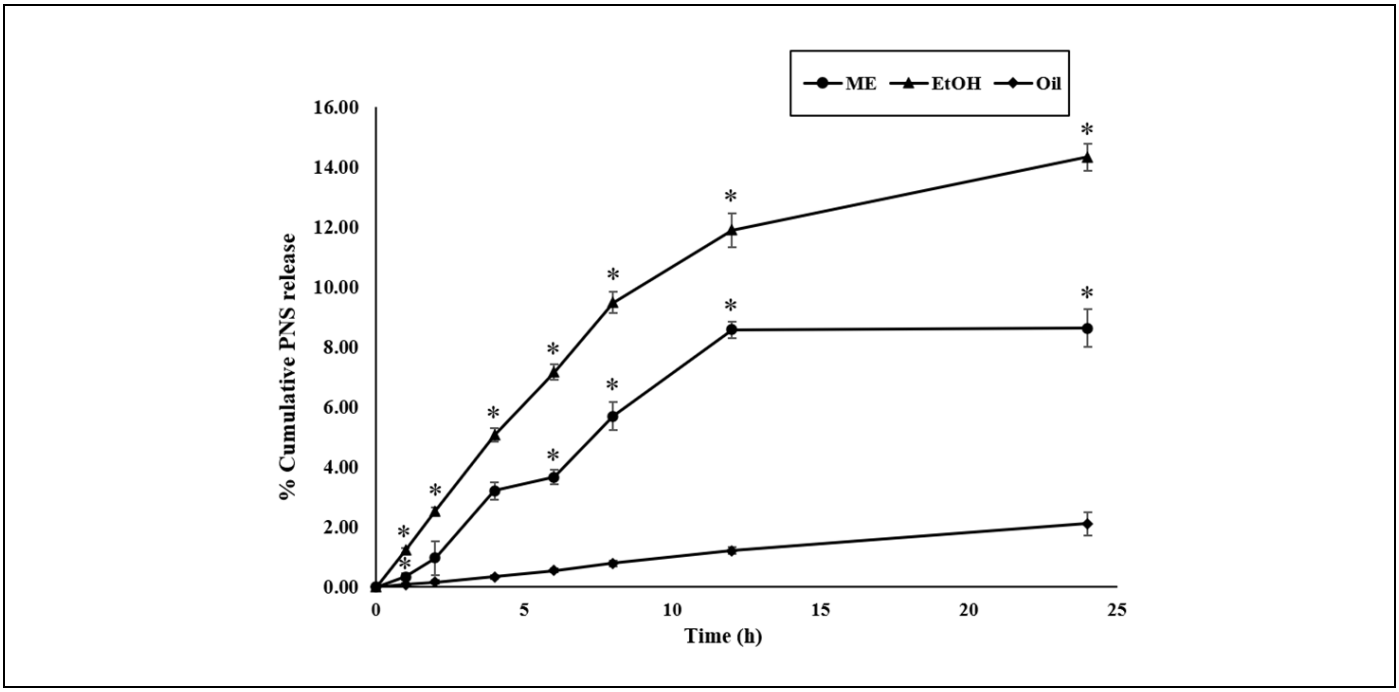

Figure 3. *In vitro* release profiles of PNS from ME (●), ethanol (▲) and oil (◆) at 24 h. Data are presented as the mean ± S.D. (n=3). * mentioned a significant difference relative to the oil formulation (*p*-value < 0.05).

the structural characteristics of ME. The interfacial film is formed by the surfactant and co-surfactant, which not only stabilizes the droplets but also acts as a diffusion barrier [34]. PNS molecules located near the interfacial region were released rapidly, giving rise to an initial burst, whereas the molecules that were entrapped within the droplet core diffused more slowly across the interfacial layer, resulting in a sustained release pattern of PNS [35].

3.6 *Ex vivo* skin permeation and deposition study

An *ex vivo* skin permeation study was performed to compare the transdermal delivery performance of *B. rotunda* extract from the formulations. The optimized ME formulation exhibited higher PNS permeated through and deposited in the skin than oil formulation (Figure 4). Although the ethanol formulation exhibited the highest release of PNS (Figure 3) and enhanced skin permeation and deposition (data not shown) by acting as a skin penetration enhancer, its application may be limited due to the potential risk of skin irritation and contact dermatitis commonly associated with ethanol [36]. The *B. rotunda* extract dissolved in the oil formulation exhibited the lowest ability to deliver PNS into and through the skin, suggesting that the lipophilic nature of the oil limited PNS release and skin permeation. The absence of a permeation-enhancing effect, combined

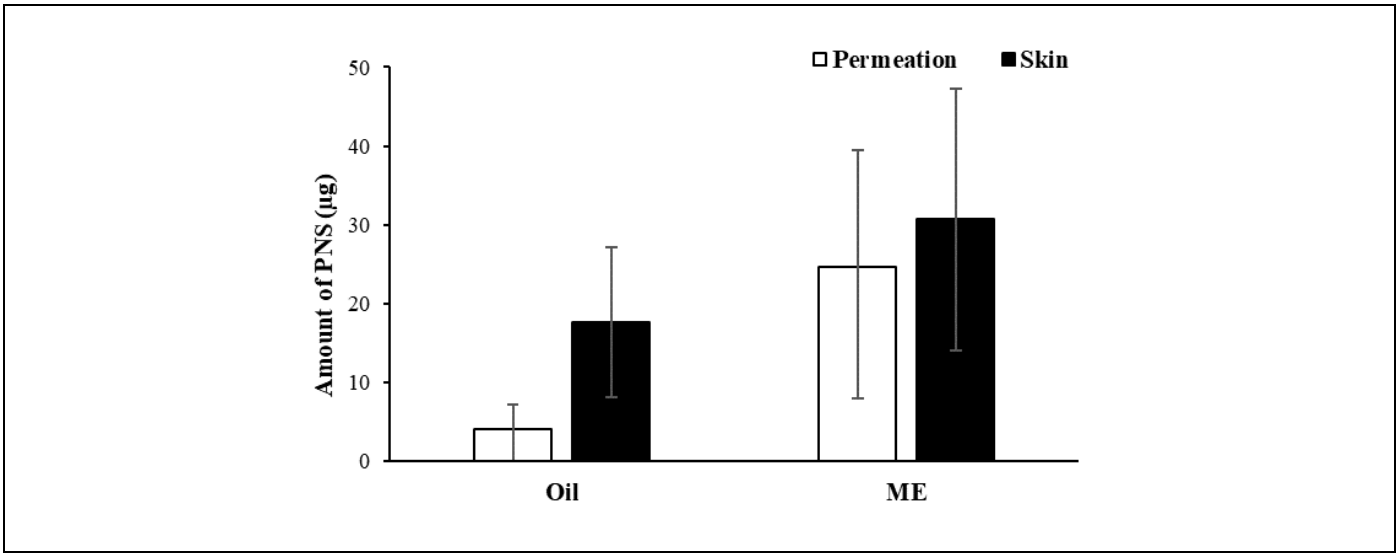

Figure 4. Skin permeation and deposition of PNS from the oil and ME formulation at 24 h. Data are presented as the mean ± S.D. (n=3).

with poor partitioning into the medium, likely explains the limited delivery observed with the oil formulation [37]. The optimized ME formulation improved the skin permeability of PNS by facilitating its passage through the stratum corneum, thereby enhancing transdermal delivery.

These MEs contain optimized oil (D-limonene), surfactant (Labrasol®)/co-surfactant (Transcutol®) and water, along with the small droplet size, acting as permeation enhancers and potentially enhancing the skin permeation and deposition [38]. D-limonene acts as a skin penetration enhancer, and its incorporation into nanovesicles has been reported to modify the lipid chain conformation in the stratum corneum and increase lipid lamellae fluidity, thereby improving skin permeability [38]. As a non-ionic surfactant, Labrasol® facilitates skin permeation by enhancing the fluidity of the stratum corneum [37]. Transcutol®, used as the co-surfactant, is also widely recognized for its ability to enhance drug solubility, improve transdermal absorption, and promote drug retention within the skin layers [39]. The nanoscale droplet size of the ME further facilitates their transport across the skin barrier [40]. Therefore, these characteristics suggest that the optimized ME system has the potential to serve as an effective carrier for enhancing the solubility and transdermal delivery of poorly water-soluble compounds, such as PNS.

4. CONCLUSIONS

In this study, the ME system incorporating *B. rotunda* extract was successfully developed and optimized for transdermal delivery using an experimental design model. The optimized formulation, composed of d-limonene, Labrasol®, and Transcutol®, exhibited desirable physicochemical characteristics, including small droplet size, low PDI, high entrapment efficiency, and pH suitable for skin application. *In vitro* drug release and *ex vivo* permeation studies demonstrated that the ME formulation significantly enhanced PNS release and skin permeation compared to ethanol and oil formulations. These findings highlight the potential of ME systems as an effective carrier for improving solubility, permeability, and improve therapeutic efficacy of poorly water-soluble compounds, PNS.

5. ACKNOWLEDGEMENTS

The authors gratefully acknowledge the Faculty of Pharmaceutical Sciences, Ubon Ratchathani University, Ubon Ratchathani, and the Faculty of Pharmacy, Silpakorn University, Nakhon Pathom, Thailand, for providing research facilities and technical support. This research was supported by the Research and Creative Fund, Faculty of Pharmacy, Silpakorn University. Appreciation is also extended to B.S.A. Farm, Ubon Ratchathani, for supplying naturally deceased neonatal porcine skin used in this study.

Author contributions

Panatda Wittayanukullack: conceptualization, methodology, visualization, writing-original draft preparation; Praneet Opanasopit: supervision, funding acquisition; Phuvamin Suriyaaumporn: methodology; Worranan Rangsimawong: conceptualization, methodology, visualization, writing-review and editing.

Funding

None to declare.

Conflict of interest

The authors declare that there are no conflicts of interest.

Ethics approval

Ethical approval for collection granted by the Investigational Review Board (27/2568/IACUC, Animal Experimentation Ethics Committee, Ubon Ratchathani University, Ubon Ratchathani, Thailand).

Article info

Received April 11, 2025
Received in revised form September 23, 2025
Accepted September 28, 2025

REFERENCES

1. Wang Y, Wen J-J, Liu F, Peng X-J, Xu G, Zhang M-L, et al. Traditional usages, chemical metabolites, pharmacological activities, and pharmacokinetics of *Boesenbergia rotunda* (L.) Mansf.: A comprehensive review. Front Pharmacol. 2025;16:1527210. https://doi.org/10.3389/fphar.2025.1527210
2. Eng-Chong T, Yean-Kee L, Chin-Fei C, Choon-Han H, Sher-Ming W, Li-Ping CT, et al. *Boesenbergia rotunda*: from ethnomedicine to drug discovery. Evid Based Complement Alternat Med. 2012;2012(1):473637. https://doi.org/10.1155/2012/473637
3. Rithichai P, Jirakiattikul Y, Poljan P, Youngvises N, Itharat A. Growth, bioactive compound accumulation and antioxidant activity in rhizomes and storage roots of *Boesenbergia rotunda* (L.) Mansf. Agr. Nat. Resour. 2022;56(2):299–306. https://li01.tci-thaijo.org/index.php/anres/article/view/254482
4. Kongsui R, Surapinit S, Promsrisuk T, Thongrong S. Pinostrobin from *Boesenbergia rotunda* attenuates oxidative stress and promotes functional recovery in rat model of sciatic nerve crush injury. Braz J Med Biol Res. 2023;56:e12578. https://doi.org/10.1590/1414-431X2023e12578
5. Han C, Raksat A, Atanu MSH, Chang LK, Wall MM, Chang LC. Investigation of antimicrobial, antioxidant, and cytotoxic activities of *Boesenbergia rotunda* rhizome extract. J. Curr. Sci. Technol. 2024;14(1):20. https://doi.org/10.1590/1414-431X2023e12578
6. Liana D, Eurtivong C, Phanumartwiwath A. *Boesenbergia rotunda* and its pinostrobin for atopic dermatitis: dual 5-lipoxygenase and cyclooxygenase-2 inhibitor and its mechanistic study through steady-state kinetics and molecular modeling. Antioxidants. 2024;13(1):74. https://doi.org/10.3390/antiox13010074
7. Abdelwahab SI, Mohan S, Abdulla MA, Sukari MA, Abdul AB, Taha MME, et al. The methanolic extract of *Boesenbergia rotunda* (L.) Mansf. and its major compound pinostrobin induces

anti-ulcerogenic property *in vivo*: possible involvement of indirect antioxidant action. J Ethnopharmacol. 2011;137(2):963-70. https://doi.org/10.1016/j.jep.2011.07.010
8. Zhao L, Yao L, Chen R, He J, Lin T, Qiu S, et al. Pinostrobin from plants and propolis against human coronavirus HCoV-OC43 by modulating host AHR/CYP1A1 pathway and lipid metabolism. Antiviral Res. 2023;212:105570. https://doi.org/10.1016/j.antiviral.2023.105570.
9. Chutiwitoonchai N, Akkarawongsapat R, Chantawarin S, Jiarpinitnun C, Liwnaree B, Teeravechyan S, et al. Antiviral effect of pinostrobin, a bioactive constituent of *Boesenbergia rotunda*, against porcine epidemic diarrhea virus. Antiviral Res. 2025;234:106073. https://doi.org/10.1016/j.antiviral.2024.106073
10. San HT, Khine HEE, Sritularak B, Prompetchara E, Chaotham C, Che C-T, et al. Pinostrobin: An adipogenic suppressor from fingerroot (*Boesenbergia rotunda*) and its possible mechanisms. Foods. 2022;11(19):3024. https://doi.org/10.3390/foods11193024
11. Gu C, Fu L, Yuan X, Liu Z. Promoting effect of pinostrobin on the proliferation, differentiation, and mineralization of murine pre-osteoblastic MC3T3-E1 cells. Molecules. 2017;22(10):1735. https://doi.org/10.3390/molecules22101735
12. Yusuf NA, M Annuar MS, Khalid N. Existence of bioactive flavonoids in rhizomes and plant cell cultures of' *Boesenbergia rotund* (L.) Mansf. Kulturpfl. Aust. J. Crop Sci. 2013;7(6):730-4. http://www.cropj.com/khalid_7_6_2013_730_734.pdf
13. Thongrong S, Surapinit S, Promsrisuk T, Jittiwat J, Kongsui R. Pinostrobin alleviates chronic restraint stress-induced cognitive impairment by modulating oxidative stress and the function of astrocytes in the hippocampus of rats. Biomed Rep. 2023;18(3):20. https://doi.org/10.3892/br.2023.1602
14. Le Bail JC, Aubourg L, Habrioux G. Effects of pinostrobin on estrogen metabolism and estrogen receptor transactivation. Cancer Lett. 2000;156(1):37-44. https://doi.org/10.1016/s0304-3835(00)00435-3
15. Saah S, Siriwan D, Trisonthi P, Dueramae S. Physicochemical and biological properties of encapsulated *Boesenbergia rotunda* extract with different wall materials in enhancing antioxidant, mineralogenic and osteogenic activities of MC3T3-E1 cells. Saudi Pharm J. 2024;32(4):101998. https://doi.org/10.1016/j.jsps.2024.101998
16. Ramadon D, McCrudden MTC, Courtenay AJ, Donnelly RF. Enhancement strategies for transdermal drug delivery systems: current trends and applications. Drug Deliv Transl Res. 2022;12(4):758-91. https://doi.org/10.1007/s13346-021-00909-6
17. Liu S, Deng T, Cheng H, Lu J, Wu J. Advances in transdermal drug delivery systems and clinical applications in inflammatory skin diseases. Pharmaceutics. 2025;17(6):746. https://doi.org/10.3390/pharmaceutics17060746
18. Karthikeyan E, Sivaneswari S. Advancements in transdermal drug delivery systems: Enhancing medicine with pain-free and controlled drug release. AI-Pharm. 2025;3(4):277-95. https://doi.org/10.1016/j.ipha.2024.09.008
19. Vaseem RS, D'cruz A, Shetty S, - H, Vardhan A, R SS, et al. Transdermal drug delivery systems: a focused review of the physical methods of permeation enhancement. Adv Pharm Bull. 2023;14(1):67. https://doi.org/10.34172/apb.2024.018
20. Abdoh A, Liu D, Mohammed Y. Enhancement of drug permeation across skin through stratum corneum ablation. RSC Pharm. 2024;1(2):151-60. https://doi.org/10.1039/D4PM00089G
21. Alkrad JA, Assaf SM, Hussein-Al-Ali SH, Alrousan R. Microemulsions as nanocarriers for oral and transdermal administration of enoxaparin. J Drug Deliv Sci Technol. 2022;70:103248. https://doi.org/10.1016/j.jddst.2022.103248
22. Souto EB, Cano A, Martin s-Gomes C, Coutinho TE, Zielińska A, Silva AM. Microemulsions and nanoemulsions in skin drug delivery. Bioengineering. 2022;9(4):158. https://doi.org/10.3390/bioengineering9040158
23. Berkman MS, Güleç K. Pseudo-ternary phase diagrams: a practical approach for the area and centroid calculation of stable microemulsion regions. Istanbul J Pharm. 2021;51(1):42-9. https://dergipark.org.tr/en/pub/iujp/issue/62349/938048
24. Sritananuwat P, Samseethong T, Jitsaeng K, Duangjit S, Opanasopit P, Rangsimawong W. Effectiveness and safety of *Boesenbergia rotunda* extract on 3T3-L1 preadipocytes and its use in capsaicin-loaded body-firming formulation: *in vitro* biological study and *in vivo* human study. Cosmetics. 2024;11(1):24. https://doi.org/10.3390/cosmetics11010024
25. Jitsaeng K, Duangjit S, Sritananuwat P, Tansathien K, Opanasopit P, Rangsimawong W. Potential lipolytic effect of panduratin A loaded microspicule serum as a transdermal delivery approach for subcutaneous fat reduction. Biol Pharm Bull. 2023;46(12):1761-8. https://doi.org/10.1248/bpb.b23-00491
26. Zhang J, Froelich A, Michniak-Kohn B. Topical delivery of meloxicam using liposome and microemulsion formulation approaches. Pharmaceutics. 2020;12(3):282. https://doi.org/10.3390/pharmaceutics12030282
27. Rangsimawong W, Jitsaeng K, Duangjit S, Sritananuwat P, Opanasopit P. Development of isolated panduratin A-loaded solid lipid nanoparticles as a transdermal delivery system for cosmeceutical products. Sci. Eng. Health Stud. 2023;17:23050003. https://doi.org/10.69598/sehs.17.23050003
28. Ramkar S, Suresh PK. Finasteride-loaded nano-lipidic carriers for follicular drug delivery: preformulation screening and Box-Behnken experimental design for optimization of variables. Heliyon. 2022;8(8):e10175. https://doi.org/10.1016/j.heliyon.2022.e10175
29. Ramalho ÍMdM, Bezerra GS, Ostrosky EA, Ferrari M, Oliveira VdS, Wanderley Neto AdO, et al. Chrysin-loaded microemulsion: formulation design, evaluation and antihyperalgesic activity in mice. Appl. Sci. 2022;12(1):477. https://doi.org/10.3390/app12010477
30. Pathuri R, Gottemukkula LD. Development and optimization of a self-nanoemulsifying drug delivery system (SNEDDS) for enhanced oral delivery of dolutegravir. J. Pharm. Innov. 2025;20(2):1-17. https://doi.org/10.1007/s12247-025-09951-0
31. Đekić L, Ćirić A, Milinković S, Budinčić JM, Fraj J, Petrović L. Film-forming microemulsions with essential oils: elucidating relationships between formulation parameters, thermodynamic stability, and quality attributes. Processes. 2025;13(4):990. https://doi.org/10.3390/pr13040990
32. McCartney F, Jannin V, Chevrier S, Boulghobra H, Hristov DR, Ritter N, et al. Labrasol® is an efficacious intestinal permeation enhancer across rat intestine: *ex vivo* and *in vivo* rat studies. J Control Release. 2019;310:115-26. https://doi.org/10.1016/j.jconrel.2019.08.008
33. Agubata CO, Nzekwe IT, Obitte NC, Ugwu CE, Attama AA, Onunkwo G. Effect of oil, surfactant and co-surfactant concentrations on the phase behavior, physicochemical properties and drug release from self-emulsifying drug delivery systems. J Drug Discov Develop and Deliv. 2014;1(1):1-7. https://austinpublishinggroup.com/drug-development/fulltext/drug-v1-id1005.php
34. Hegde RR, Verma A, Ghosh A. Microemulsion: new insights into the ocular drug delivery. ISRN Pharm. 2013;(1):826798. https://doi.org/10.1155/2013/826798
35. Sarheed O, Dibi M, Ramesh KVRNS, Drechsler M. Fabrication of alginate-based O/W nanoemulsions for transdermal drug delivery of lidocaine: influence of the oil phase and surfactant. Molecules. 2021;26(9):2556. https://doi.org/10.3390/molecules26092556 .
36. Lachenmeier DW. Safety evaluation of topical applications of ethanol on the skin and inside the oral cavity. J Occup Med Toxicol. 2008;3(26):1-16. https://doi.org/10.1186/1745-6673-3-26
37. Nokhodchi A, Shokri J, Dashbolaghi A, Hassan-Zadeh D, Ghafourian T, Barzegar-Jalali M. The enhancement effect of

surfactants on the penetration of lorazepam through rat skin. Int J Pharm. 2003;250(2):359-69. https://doi.org/10.1016/S0378-5173(02)00554-9

38. Rangsimawong W, Obata Y, Opanasopit P, Ngawhirunpat T, Takayama K. Enhancement of galantamine HBr skin permeation using sonophoresis and limonene-containing PEGylated liposomes. AAPS PharmSciTech. 2018;19:1093-104. https://doi.org/10.1208/s12249-017-0921-z
39. Osborne DW, Musakhanian J. Skin penetration and permeation properties of Transcutol®-neat or diluted mixtures. AAPS PharmSciTech. 2018;19:3512-33. https://doi.org/10.1208/s12249-018-1196-8
40. Virani A, Dholaria N, Matharoo N, Michniak-Kohn B. A study of microemulsion systems for transdermal delivery of risperidone using penetration enhancers. J Pharm Sci. 2023;112(12): 3109-19. https://doi.org/10.1016/j.xphs.2023.07.007